

DOI: 10.1002/ange.200603651

**Isolated  $[\text{Ni}_2\text{H}_7]^{7-}$  and  $[\text{Ni}_4\text{H}_{12}]^{12-}$  Ions in  $\text{La}_2\text{MgNi}_2\text{H}_8^{**}$** *Jean-Noël Chotard, Yaroslav Filinchuk, Bernard Revaz, and Klaus Yvon\**

Solid-state metal hydrides provide a safe and efficient way of storing hydrogen. Those useful for applications in the energy sector, such as proton-exchange membrane (PEM) fuel cells, are mainly derived from stable intermetallic compounds and alloys. These hydrides are usually metallic and nonstoichiometric, and are called “interstitial” because hydrogen atoms occupy interstices in the metal-atom network. “Complex” metal hydrides form a distinctly different class of materials. Their name is derived from the presence of discrete metal-hydrogen complexes (where the metal is a p- or d-block element) in the structures, for example, the iron-based  $[\text{FeH}_6]^{4-}$  ions in  $\text{Mg}_2\text{FeH}_6$  or the aluminum-based  $[\text{AlH}_4]^-$  ions in  $\text{NaAlH}_4$ . These hydrides are not derived from stable intermetallic compounds and are usually stoichiometric and nonmetallic.

Among the hydrides based on d-block elements, the first member and textbook example is  $\text{K}_2\text{ReH}_9$ . This compound was reported in 1964 and was found to contain tricapped trigonal-prismatic  $[\text{ReH}_9]^{2-}$  complex anions. In the 1980s, many other complex transition-metal hydrides were discovered, such as the members of the series  $\text{Mg}_2\text{FeH}_6/\text{Mg}_2\text{CoH}_5/\text{Mg}_2\text{NiH}_4$ , which contain octahedral  $[\text{FeH}_6]^{4-}$ , square-pyramidal  $[\text{CoH}_5]^{4-}$ , or tetrahedral  $[\text{NiH}_4]^{4-}$  18-electron complex anions, respectively. Since then, the number of such hydrides has continuously increased, and it now totals over 80 compounds containing some 30 different transition-metal hydride complexes.<sup>[1]</sup>

Almost all of the known solid-state transition-metal hydride complexes are mononuclear and have terminal

[\*] J.-N. Chotard, Dr. Y. Filinchuk,<sup>[†]</sup> Prof. Dr. K. Yvon  
Laboratoire de Cristallographie  
Université de Genève  
Quai Ernest Ansermet 24, 1211 Genève 4 (Switzerland)  
Fax: (+41) 223-796-108  
E-mail: klaus.yvon@cryst.unige.ch

Dr. B. Revaz  
Département de Physique de la Matière Condensée  
Université de Genève  
Quai Ernest Ansermet 24, 1211 Genève 4 (Switzerland)

[†] Current address:  
Swiss-Norwegian Beam Lines at ESRF, BP 220  
38043 Grenoble (France)

[\*\*] This work was supported by the Swiss National Science Foundation and the Swiss Federal Office of Energy. We thank Dr. Nick Clayton (Siemens, Oxon) for the electrical-resistance measurements and Jean-Luc Lorenzoni (Geneva) for technical help.



Supporting information for this article is available on the WWW under <http://www.angewandte.org> or from the author.

hydride ligands. Polynuclear hydride complexes with bridging hydride ligands are less common, but are of considerable interest because of possible links to interstitial hydrides. An example involving a 5d metal is the dinuclear  $[\text{Pt}_2\text{H}_9]^{5-}$  complex anion in  $\text{Li}_5\text{Pt}_2\text{H}_9$ , which contains a linear Pt–H–Pt bond.<sup>[2]</sup> No examples of polynuclear solid-state complexes involving 3d metals have yet been reported. Likewise, hydride structures containing more than one type of transition-metal complex are very rare. The only known cases are  $\text{Mg}_6\text{T}_2\text{H}_{11}$  ( $\text{T} = \text{Co},^{[3]} \text{Ir}^{[4]}$ ), which contain partially disordered square-pyramidal  $[\text{TH}_3]^{4-}$  and saddle-like  $[\text{TH}_4]^{5-}$  complex anions.

Herein, we report the discovery of the first polynuclear solid-state hydride complexes of a 3d metal, nickel. The only previously known solid-state nickel hydride complex is the mononuclear tetrahedral 18-electron  $[\text{NiH}_4]^{4-}$  anion, which occurs in  $\text{Mg}_2\text{NiH}_4$ ,  $\text{MMgNiH}_4$  ( $\text{M} = \text{Ca}, \text{Sr}, \text{Eu}, \text{Yb}$ ), and the recently reported  $\text{LaMg}_2\text{NiH}_7$ .<sup>[5]</sup> The compound described herein,  $\text{La}_2\text{MgNi}_2\text{H}_8$ , belongs to the same system, and contains a fully ordered arrangement of isolated dinuclear  $[\text{Ni}_2\text{H}_7]^{7-}$  and tetranuclear  $[\text{Ni}_4\text{H}_{12}]^{12-}$  complexes. Furthermore, its formation is associated with a hydrogen-induced metal–insulator transition, which is a relatively rare phenomenon in transition-metal–hydrogen systems.

The new compound  $\text{La}_2\text{MgNi}_2\text{H}_8$  can be obtained readily by hydrogenation of the intermetallic compound  $\text{La}_2\text{MgNi}_2$ ,<sup>[6]</sup> which crystallizes in the tetragonal  $\text{Mo}_2\text{FeB}_2$  structure type. Hydrogenation in an autoclave at a temperature of 100 °C and a pressure of 30 bar over 24 h yields single-phase samples in a fairly reproducible manner. The analogous deuteride forms under the same conditions. For 10 samples, no significant variation of the cell parameters or hydrogen content was observed. Thus, the hydride can be considered as an essentially stoichiometric compound. The mass increase during hydrogenation corresponds to a hydrogen content of approximately eight hydrogen atoms per formula unit, that is, to a composition of  $\text{La}_2\text{MgNi}_2\text{H}_8$ . The corresponding weight and volume efficiencies for hydrogen storage are 1.89 wt% and 97 g L<sup>−1</sup>. During hydrogenation, the host structure undergoes a monoclinic distortion and a lattice expansion of  $\Delta V/V \approx 20\%$ .<sup>[7]</sup> Attempts to desorb the hydride ligands under technically accessible conditions were unsuccessful. The application of a vacuum (ca.  $1 \times 10^{-3}$  bar) while heating at 300 °C over 24 h led to a partial segregation into the binary hydride  $\text{LaH}_3$  and a secondary phase. Thus,  $\text{La}_2\text{MgNi}_2\text{H}_8$  should be considered as a nonreversible hydride, with respect to the conditions typical of possible applications in the energy sector.

The structure of  $\text{La}_2\text{MgNi}_2\text{H}_8$  was determined from synchrotron X-ray and neutron diffraction data collected for powder samples of the deuteride. In  $\text{La}_2\text{MgNi}_2\text{D}_8$ , the arrangement of the metal atoms is very similar to that in hydrogen-free  $\text{La}_2\text{MgNi}_2$ , the maximum atomic shifts being approximately 0.65 Å. The deuterium atoms fall into two classes, depending on whether or not they are bonded to nickel atoms. As shown in Figure 1, those bonded to nickel atoms (D11–D14, D21–D24, D31, D32, D41–D43) form two sorts of polynuclear nickel–deuterium complexes (**I**, **II**). All of the nickel atoms are surrounded by terminal (D11, D14, D21, D22, D24, D31, D32, D41–D43) and bridging (D12,

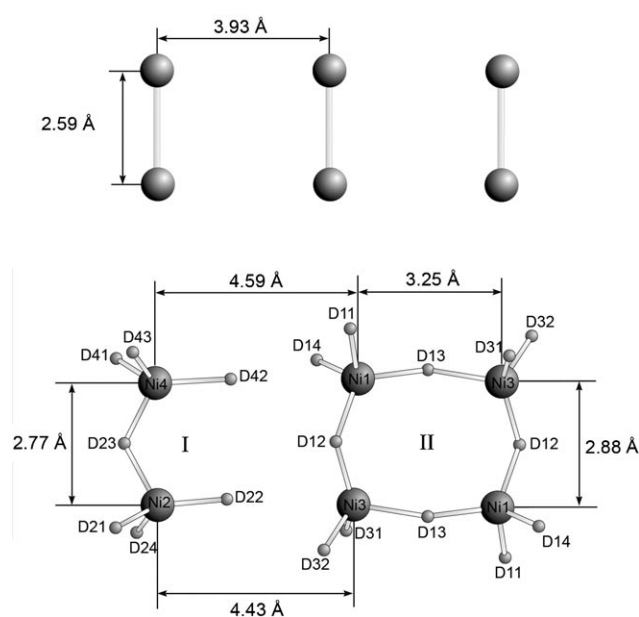


**Figure 1.** Arrangement of the  $[\text{Ni}_2\text{D}_7]^{7-}$  (**I**) and  $[\text{Ni}_4\text{D}_{12}]^{12-}$  (**II**) complex anions in the structure of  $\text{La}_2\text{MgNi}_2\text{D}_8$  (bottom), and comparison with the arrangement of the nickel atoms in  $\text{La}_2\text{MgNi}_2$  (top).

D13, D23) deuteride ligands in approximately tetrahedral configurations.

The dinuclear  $[\text{Ni}_2\text{D}_7]^{7-}$  complex **I** consists of a pair of nickel-centered ( $\text{Ni}_2$ ,  $\text{Ni}_4$ ) tetrahedra, which share a corner (D23). The tetranuclear  $[\text{Ni}_4\text{D}_{12}]^{12-}$  complex **II** consists of four nickel-centered ( $2\text{Ni}_1$ ,  $2\text{Ni}_3$ ) tetrahedra, which each share two corners (D12, D13). Given that the Ni–D distances within the complexes (**I**: Ni–D 1.52–1.71 Å, **II**: Ni–D 1.50–1.70 Å) are much shorter than those between the complexes ( $\text{Ni}_3$ –D22 2.86 Å,  $\text{Ni}_1$ –D42 2.88 Å), the complexes are well-isolated from one another. The D–Ni–D bond angles deviate from the ideal tetrahedral angle of 109° (terminal: D–Ni–D 92–129°, bridging:  $\text{Ni}_1$ –D13– $\text{Ni}_3$  157°,  $\text{Ni}_1$ –D12– $\text{Ni}_3$  127°,  $\text{Ni}_2$ –D23– $\text{Ni}_4$  125°). In particular, the  $\text{Ni}_2$ –D23– $\text{Ni}_4$  bridge in **I** is significantly opened, but much less so than the linear Pt–H–Pt bridge found in the dinuclear  $[\text{Pt}_2\text{H}_9]^{5-}$  complex of  $\text{Li}_5\text{Pt}_2\text{H}_9$ .<sup>[2]</sup>

The stereochemical activity of the deuteride ligands is not only apparent from the bond angles, but also from the changes in the Ni–Ni distances that are induced by deuteration. While the nickel atoms in the deuterium-free compound are arranged in equidistant pairs (intrapair: Ni–Ni 2.59 Å, interpair: Ni–Ni 3.93 Å; Figure 1, top), those in the deuteride are rearranged, such that the distances between the nickel pairs in **II** ( $\text{Ni}_1$ – $\text{Ni}_3$  3.25 Å) are considerably shortened (Figure 1, bottom), owing to the presence of bridging deuteride ligands (D13). On the other hand, the Ni–Ni distances between the pairs in **I** and **II** are much longer ( $\text{Ni}_2$ – $\text{Ni}_3$  4.43 Å,  $\text{Ni}_1$ – $\text{Ni}_4$  4.59 Å), owing to the absence of bridging deuteride ligands. The distances within the nickel pairs are lengthened in both complexes (**I**:  $\text{Ni}_2$ – $\text{Ni}_4$  2.77 Å, **II**:  $\text{Ni}_1$ – $\text{Ni}_3$  2.88 Å), owing to the presence of the bridging ligands D23 and D12. Finally, the Ni–D distances involving the terminal deuterium atoms are slightly shorter on average

(Ni–D 1.58 Å) than those involving the bridging deuterium atoms (Ni–D 1.61 Å), and compare well with those in the mononuclear  $[\text{NiD}_4]^{4-}$  complexes of other complex metal hydrides, such as  $\text{LaMg}_2\text{NiD}_7$  (Ni–D 1.58 Å),  $\text{Mg}_2\text{NiD}_4$  (Ni–D 1.54 Å) and  $\text{CaMgNiD}_4$  (Ni–D 1.60 Å). The three remaining deuterium atoms in the structure are not bonded to nickel atoms and have octahedral  $\text{La}_4\text{Mg}_2$  or tetrahedral  $\text{La}_2\text{Mg}_2$  coordination environments.

When considered together, the structural features suggest a bonding description in terms of  $\text{La}^{3+}$  and  $\text{Mg}^{2+}$  cations, and  $[\text{Ni}_2\text{H}_7]^{7-}$ ,  $[\text{Ni}_4\text{H}_{12}]^{12-}$ , and  $\text{H}^-$  anions. The corresponding limiting ionic formula is  $4\text{La}_2\text{MgNi}_2\text{H}_8 = 8\text{La}^{3+} + 4\text{Mg}^{2+} + [\text{Ni}_4\text{H}_{12}]^{12-} + 2[\text{Ni}_2\text{H}_7]^{7-} + 6\text{H}^-$ . In this picture, the electronic requirements of the nickel atoms in each complex anion (**I**: 34 electrons, **II**: 64 electrons) can be rationalized in terms of the 18-electron rule by attributing two-centre two-electron (2c-2e) bonds to the terminal hydrogen atoms, and three-center two-electron (3c-2e) bonds to the bridging hydrogen atoms. This model implies that the nickel atoms are essentially zero-valent and have  $\text{sp}^3$ -hybridized valence orbitals; that is, the nickel d bands are filled, and the compound is possibly diamagnetic and insulating.

While the intermetallic compound  $\text{La}_2\text{MgNi}_2$  has a very low electrical resistance, consistent with metallic behavior, the hydride is clearly semiconducting. However, owing to the inability to compact the powder samples sufficiently, a reliable value for the band gap could not be obtained. Magnetic measurements revealed that  $\text{La}_2\text{MgNi}_2\text{H}_8$  is slightly ferromagnetic, rather than diamagnetic as expected. Samples of both the intermetallic compound and the hydride exhibited a small hysteresis, and the saturation moment of the hydride (ca.  $0.096 \text{ emu g}^{-1}$  at 2 K) was approximately twice as large as that of the hydrogen-free compound (ca.  $0.044 \text{ emu at 2 K}$ ). This behavior is probably due to traces of ferromagnetic nickel that were not detected by X-ray diffraction ( $\text{La}_2\text{MgNi}_2$ : ca. 0.25 wt %,  $\text{La}_2\text{MgNi}_2\text{H}_8$ : ca. 0.77 wt %; as estimated from the saturation magnetization). Additional nickel may have been formed at the grain boundaries during hydrogenation. This so-called “surface segregation” effect has been observed in related metal–hydrogen systems, such as  $\text{LaNi}_5\text{–H}$ ,<sup>[8]</sup> and presumably masks the expected diamagnetism of  $\text{La}_2\text{MgNi}_2\text{H}_8$ .

In conclusion, we have reported the first case of a solid-state metal hydride containing polynuclear hydride complexes of a 3d metal. In contrast to the known nickel-based metal hydrides, which contain exclusively mononuclear tetrahedral  $[\text{NiH}_4]^{4-}$  complexes with terminal hydride ligands,  $\text{La}_2\text{MgNi}_2\text{H}_8$  contains (fully ordered) dinuclear  $[\text{Ni}_2\text{H}_7]^{7-}$  and tetranuclear  $[\text{Ni}_4\text{H}_{12}]^{12-}$  complexes with both terminal and bridging hydride ligands. The geometries of the complexes are unique for complex metal hydrides, and remotely resemble those of the  $[\text{Si}_2\text{O}_7]^{6-}$  and  $[\text{Si}_4\text{O}_{12}]^{8-}$  anions in soro- and ring silicates, respectively.

The nonmetallic character of  $\text{La}_2\text{MgNi}_2\text{H}_8$  presumably results from the condensation of valence electrons into metal–hydrogen bonds in  $[\text{Ni}_2\text{H}_7]^{7-}$  and  $[\text{Ni}_4\text{H}_{12}]^{12-}$  anions having closed-shell electron configurations (18 electrons per nickel atom). This is the fourth example of a hydrogenation-induced metal–nonmetal transition in a transition-metal–hydrogen

system. In all four cases, metallic compounds ( $\text{Mg}_2\text{Ni}$ ,  $\text{Mg}_3\text{Ir}$ ,  $\text{LaMg}_2\text{Ni}$ , and  $\text{La}_2\text{MgNi}_2$ ) transform into nonmetallic hydrides (brownish-red  $\text{Mg}_2\text{NiH}_4$ , red  $\text{Mg}_6\text{Ir}_2\text{H}_{11}$ , dark gray  $\text{LaMg}_2\text{NiH}_7$ , and  $\text{La}_2\text{MgNi}_2\text{H}_8$ ) containing transition-metal hydride complexes. Such transitions are of both fundamental and technological interest. They shed new light on metal–hydrogen interactions at the frontier between covalently bonded and metallic systems.

While the hydrogen-atom positions and hydrogen contents of covalently bonded systems can be rationalized in terms of covalent bonds (for example, 2c-2e) with directional character (for example,  $\text{sp}^3$ ) and in terms of closed-shell electron configurations (for example, 18 electrons), those in metallic systems cannot. Hydrogen in metallic systems is generally considered as a stereochemically inert species that occupies the available interstices in the metal-atom framework on purely geometric grounds; hence, such systems are called “interstitial” hydrides. While such a description allows the prediction of some possible hydrogen sites, it generally does not allow the rationalization of all possible hydrogen sites and, thus, hydrogen contents. Clearly, directional bonding around the transition metals, charge transfer, and valence-electron counts must be considered as well. Furthermore, systems at the border between metallic and insulating are of interest for practical applications, such as optical mirrors (for example,  $\text{Mg}_2\text{Co–H}$ <sup>[9]</sup> and other systems<sup>[10]</sup>) and hydrogen detectors. These applications require, however, systems that are reversible at practical temperatures. Thus, a future challenge is the investigation of additional transition-metal–hydrogen systems, in particular those likely to contain polynuclear and/or heteronuclear complex anions that are fully reversible. The prospects of finding such complexes are good, since the possible element combinations are numerous and have not yet been fully explored.

## Experimental Section

**Synthesis:** Samples of nominal composition  $\text{La}_2\text{MgNi}_2$  were synthesized by sintering arc-melted  $\text{LaNi}$  with elemental magnesium in sealed tantalum tubes. The tubes were placed in a resistance furnace and annealed under vacuum for 2 h at  $400^\circ\text{C}$ , then for 2 h at  $600^\circ\text{C}$ , and finally for 3 h at  $680^\circ\text{C}$ . The resulting samples were single-phase, according to powder X-ray diffraction. Samples of  $\text{La}_2\text{MgNi}_2\text{H}_8$  and  $\text{La}_2\text{MgNi}_2\text{D}_8$  were prepared by activating a powder sample of  $\text{La}_2\text{MgNi}_2$  under vacuum at  $100^\circ\text{C}$  for 14 h and then heating it with 30 bar of hydrogen or deuterium gas for 24 h at  $100^\circ\text{C}$  in an autoclave.

**Powder synchrotron X-ray diffraction:** A sample of  $\text{La}_2\text{MgNi}_2\text{D}_8$  was studied at one of the Swiss–Norwegian Beam Lines (BM01) at the ESRF (Grenoble, France). The powder sample was filled into a glass capillary (0.4-mm diameter) and was measured in Debye–Scherrer geometry:  $\lambda = 0.37504 \text{ Å}$ ,  $2\theta = 2.2\text{--}32.4^\circ$ , step size =  $0.004^\circ$ . The powder pattern was indexed (DICVOL04<sup>[11]</sup>) in a monoclinic cell, and the systematic absences were consistent with the centrosymmetric space group  $P2_1/c$ . The structure refinement was carried out with FULLPROF, starting with atomic coordinates found by FOX<sup>[12]</sup> (four lanthanum, four nickel, and two magnesium sites, all on 4a equipoint (Wyckoff) positions).

**Powder neutron diffraction:** Data were collected for a powder sample of  $\text{La}_2\text{MgNi}_2\text{D}_8$  (ca. 6 g) on the HRPT diffractometer at the SINQ of the PSI (Villigen, Switzerland) in high-intensity mode:  $\lambda = 1.8857 \text{ Å}$ ,  $2\theta = 5\text{--}164^\circ$ , step size =  $0.1^\circ$ , data collection time  $\approx 12 \text{ h}$ . The deuterium atoms were found using FOX.<sup>[12]</sup> Sixteen deuterium-

atom sites were located on 4a equipoint (Wyckoff) positions in space group  $P2_1/c$ , consistent with the composition  $\text{La}_2\text{MgNi}_2\text{D}_8$ , and were subsequently refined by the Rietveld method.

**Electrical resistance:** Electrical-resistance measurements were made on a pressed-powder pellet of  $\text{La}_2\text{MgNi}_2\text{H}_8$  ( $10 \times 4 \times 1 \text{ mm}^3$ ) using the four-contact technique. Voltage and current leads were attached using silver paint. The pellet was mounted on an electrically insulated support and then attached to the cold finger of a cryocooler. Data were recorded upon cooling from room temperature to 10 K in steps of 5 K with applied direct currents of  $1 \times 10^{-4}$ – $1 \times 10^{-8} \text{ A}$  during three consecutive runs.

**Magnetism:** The magnetic properties of  $\text{La}_2\text{MgNi}_2$  and  $\text{La}_2\text{MgNi}_2\text{H}_8$  were studied on a MPMS SQUID magnetometer. Magnetization curves were measured for pressed-powder samples (ca. 200 mg) at 2, 10, and 50 K. The maximum applied field was 5.5 T. To avoid ferromagnetic contamination, samples were prepared from very pure starting elements (nickel powder and magnesium pieces, 99.999 %, Sigma-Aldrich; lanthanum pieces containing 5.22 ppm iron, 0.56 ppm nickel, and 0.09 ppm cobalt, Ames Laboratory). From the stated purities, the total amount of iron and other metal impurities was estimated to be less than 27 ppm.

Further experimental details, diffraction patterns, crystallographic data, interatomic distances, electrical-resistance data, and magnetic data are given in the Supporting Information.

Received: September 6, 2006

Published online: November 7, 2006

**Keywords:** electrical properties · hydride ligands · hydrides · neutron diffraction · nickel

- 
- [1] For a recent review: K. Yvon, G. Renaudin in *Encyclopedia of Inorganic Chemistry*, 2nd ed. (Ed.: R. B. King), Wiley, New York, **2005**, pp. 1814–1846.
- [2] W. Bronger, L. à Brassard, *Angew. Chem.* **1995**, *107*, 984; *Angew. Chem. Int. Ed. Engl.* **1995**, *34*, 898.
- [3] R. Černý, F. Bonhomme, K. Yvon, P. Fischer, P. Zolliker, D. E. Cox, A. Hewat, *J. Alloys Compd.* **1992**, *187*, 233.
- [4] R. Černý, J. M. Joubert, H. Kohlmann, K. Yvon, *J. Alloys Compd.* **2002**, *340*, 180.
- [5] K. Yvon, G. Renaudin, C. M. Wei, M. Y. Chou, *Phys. Rev. Lett.* **2005**, *94*, 066403.
- [6] R.-D. Hoffmann, A. Fugmann, U. C. Rodewald, R. Pöttgen, *Z. Anorg. Allg. Chem.* **2000**, *626*, 1733.
- [7]  $\vec{a}_{\text{mono}} = \vec{a}_{\text{tetra}} + 2\vec{c}_{\text{tetra}}$ ;  $\vec{b}_{\text{mono}} = \vec{b}_{\text{tetra}}$ ;  $\vec{c}_{\text{mono}} = \vec{a}_{\text{tetra}} + 2\vec{c}_{\text{tetra}}$ ;  $\text{La}_2\text{MgNi}_2$ :  $a_{\text{tetra}} = 7.656(1)$ ,  $c_{\text{tetra}} = 3.9250(8) \text{ Å}$ ,  $V_{\text{tetra}} = 230.10(7) \text{ Å}^3$ ;  $\text{La}_2\text{MgNi}_2\text{D}_8$ :  $a_{\text{mono}} = 11.84482(1)$ ,  $b_{\text{mono}} = 7.821099(8)$ ,  $c_{\text{mono}} = 11.96310(1) \text{ Å}$ ,  $\beta = 92.780(1)^\circ$ ,  $V_{\text{mono}} = 1106.96(2) \text{ Å}^3$ .
- [8] L. Schlappbach, *J. Phys. F* **1980**, *10*, 2477.
- [9] T. J. Richardson, J. L. Slack, B. Farangis, M. D. Rubin, *Appl. Phys. Lett.* **2002**, *80*, 1349, and references therein.
- [10] R. Griessen, *Europhys. News* **2001**, *32*, 41.
- [11] A. Boulitif, D. Louër, *J. Appl. Crystallogr.* **2004**, *37*, 724.
- [12] V. Favre-Nicolin, R. Černý, *J. Appl. Crystallogr.* **2002**, *35*, 734; see also: <http://objcryst.sourceforge.net>.
-